

**Photoemission signature of the competition between magnetic order and Kondo effect in CeCoGe<sub>3</sub>**

Peng Li,<sup>1</sup> Huiqing Ye,<sup>1</sup> Yong Hu,<sup>2</sup> Yuan Fang,<sup>1</sup> Zhiguang Xiao,<sup>1</sup> Zhongzheng Wu,<sup>1</sup> Zhaoyang Shan,<sup>1</sup> Ravi P. Singh,<sup>3</sup> Geetha Balakrishnan,<sup>4</sup> Dawei Shen,<sup>5</sup> Yi-feng Yang,<sup>6</sup> Chao Cao,<sup>1</sup> Nicholas C. Plumb,<sup>2</sup> Michael Smidman,<sup>1,\*</sup> Ming Shi,<sup>2</sup> Johann Kroha,<sup>7</sup> Huiqiu Yuan,<sup>1,8,9,†</sup> Frank Steglich,<sup>1,10</sup> and Yang Liu,<sup>1,8,‡</sup>

<sup>1</sup>Center for Correlated Matter and Department of Physics, Zhejiang University, Hangzhou 310058, China

<sup>2</sup>Paul Scherrer Institute, Swiss Light Source, CH-5232 Villigen PSI, Switzerland

<sup>3</sup>Department of Physics, Indian Institute of Science Education and Research Bhopal, Bhopal 462066, India

<sup>4</sup>Department of Physics, University of Warwick, Coventry CV4 7AL, United Kingdom

<sup>5</sup>National Synchrotron Radiation Laboratory, University of Science and Technology of China, Hefei 230029, China

<sup>6</sup>Beijing National Laboratory for Condensed Matter Physics, Institute of Physics, Chinese Academy of Science, Beijing 100190, China

<sup>7</sup>Physikalisches Institut, Universität Bonn, Nussallee 12, 53115 Bonn, Germany

<sup>8</sup>Collaborative Innovation Center of Advanced Microstructures, Nanjing University, Nanjing, China

<sup>9</sup>State Key Laboratory of Silicon Materials, Zhejiang University, Hangzhou 310058, China

<sup>10</sup>Max Planck Institute for Chemical Physics of Solids, 01187 Dresden, Germany



(Received 24 August 2022; revised 23 March 2023; accepted 21 April 2023; published 4 May 2023)

The competition between magnetic order and Kondo effect is essential for the rich physics of heavy fermion systems. Nevertheless, how such competition is manifested in the quasiparticle bands in a real periodic lattice remains elusive in spectroscopic experiments. Here we report a high-resolution photoemission study of the antiferromagnetic Kondo lattice system CeCoGe<sub>3</sub> with a high  $T_{N1}$  of 21 K. Our measurements reveal a weakly dispersive  $4f$  band at the Fermi level near the  $Z$  point, arising from a moderate Kondo effect. The intensity of this heavy  $4f$  band exhibits a logarithmic increase with lowering temperature and begins to deviate from this Kondo-like behavior below  $\sim 25$  K, just above  $T_{N1}$ , and eventually ceases to grow below  $\sim 12$  K. Our work provides direct spectroscopic evidence for the competition between magnetic order and the Kondo effect in a Kondo lattice system with local-moment antiferromagnetism, indicating a distinct scenario for the microscopic coexistence and competition of these phenomena, which might be related to the real-space modulation.

DOI: [10.1103/PhysRevB.107.L201104](https://doi.org/10.1103/PhysRevB.107.L201104)

Heavy-fermion (HF) compounds are prototypical strongly correlated electron systems and host many intriguing electronic phases, including Fermi liquids with extremely heavy quasiparticles, quantum criticality, non-Fermi-liquid behavior, and unconventional superconductivity [1–7]. Lying at the heart of the rich physics in HF systems is the competition between the Ruderman-Kittel-Kasuya-Yosida (RKKY) magnetic exchange interaction [8–10] and the many-body Kondo effect [1,11–15]. Although both interactions stem from the same spin-exchange coupling  $J$  between the conduction electrons and local moments, the strengths of these interactions exhibit distinct dependences on  $J$ , leading to a magnetically ordered (paramagnetic) ground state at small (large)  $J$ . Their competition is manifested in the Doniach phase diagram [16], which underlies the phase diagrams of many HF compounds upon tuning with parameters such as pressure or chemical doping.

Of particular interest is the nature of the  $4f$  electrons that underlies the aforementioned competition in HF systems with different antiferromagnetic (AFM) characters, as well

as its connection with quantum criticality. In itinerant AFM systems such as CeCu<sub>2</sub>Si<sub>2</sub> [17–21], the magnetic order is mainly driven by nesting of the renormalized Fermi surface (FS) and the associated quantum critical point (QCP) is of the HF spin-density-wave (SDW) type [18,20]. On the other hand, local-moment AFM order is primarily mediated by the RKKY interaction, which often suppresses the Kondo screening and leads to the localization of  $4f$  electrons. In addition, unconventional local-type quantum criticality has been proposed in some local-moment HF systems [22–27], where the QCP is accompanied by an abrupt zero-temperature FS reconstruction, from a “small FS” without  $4f$  electrons in the AFM state to a “large FS” including  $4f$  electrons in the paramagnetic state. However, how the competition between the RKKY and Kondo interactions is manifested in the quasiparticle spectrum in a periodic Kondo lattice remains largely unexplored in electron spectroscopic experiments, e.g., angle-resolved photoemission spectroscopy (ARPES) and scanning tunneling microscopy (STM). Although it has been simulated by two-impurity Kondo systems in previous STM studies [28,29], experiments on real periodic lattices are still lacking.

One approach to directly probe this competition is to track the  $4f$  bands of an AFM HF system across (and well below) the magnetic transition using ARPES. However, due to the typically low transition temperatures in Ce-based HF systems,

\*msmidman@zju.edu.cn

†hqyuan@zju.edu.cn

‡yangliu@zju.edu.cn

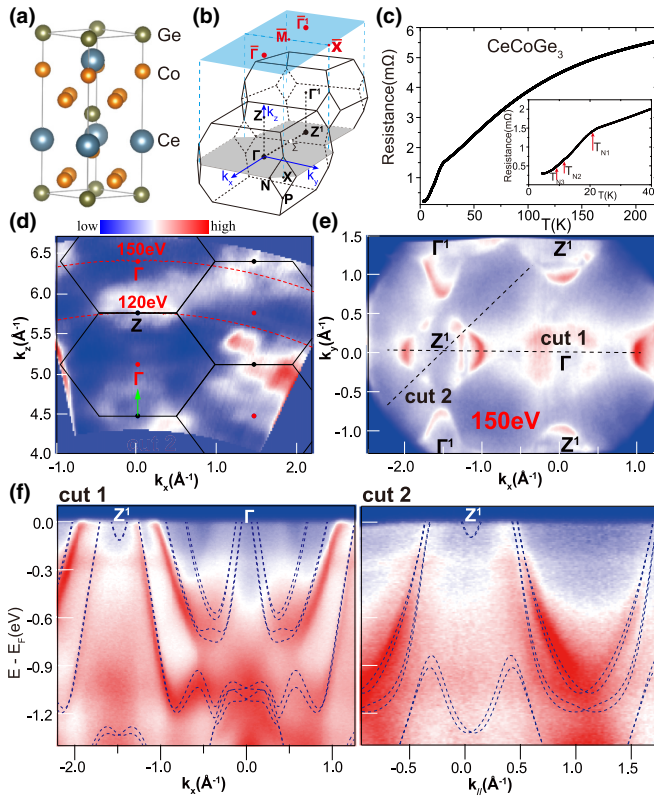


FIG. 1. (a) Crystal structure of CeCoGe<sub>3</sub>. (b) The corresponding bulk and surface BZs with high symmetry points labeled. (c) The resistance vs temperature for CeCoGe<sub>3</sub>. The inset displays an enlarged view of the low temperature region showing the AFM transitions. (d) The  $k_x - k_z$  FS map obtained from a photon-energy dependent scan (60–160 eV) at 26 K. The black hexagons indicate the bulk BZ boundaries and the dots indicate high symmetry momentum points. (e) In-plane  $k_x - k_y$  FS map obtained from 150 eV photons ( $k_z \sim 0$ ) at 5.2 K. (f) Energy-momentum dispersions along cut 1 and cut 2 shown in (e). Calculated bands (dashed blue curves) from DFT are overlaid on top.

very few studies have been reported so far [30], and signatures of such competition have not been observed. CeCoGe<sub>3</sub> is a very suitable candidate for such a study, since it shows evidence of Kondo screening already at elevated temperatures and has a reasonably high AFM ordering temperature of  $T_{N1} = 21$  K [31–33]. Here we show that CeCoGe<sub>3</sub> does show signatures of the aforementioned competition, where our systematic temperature-dependent study across the transition reveals a clear deviation from Kondo-like behaviors in the AFM phase.

CeCoGe<sub>3</sub> crystallizes in a noncentrosymmetric BaNiSn<sub>3</sub>-type structure [Fig. 1(a)], whose bulk Brillouin zone (BZ) and projected surface BZ are displayed in Fig. 1(b). The noncentrosymmetric structure can give rise to Weyl points in its correlated band structure, as predicted by calculations [34], and unconventional superconductivity with mixed singlet-triplet pairing [35,36]. The resistance [Fig. 1(c)] clearly shows kinks at 21 K ( $T_{N1}$ ), 12 K ( $T_{N2}$ ), and 8 K ( $T_{N3}$ ), which correspond to three consecutive AFM transitions [32]. Details of ARPES measurements and band structure calculations can

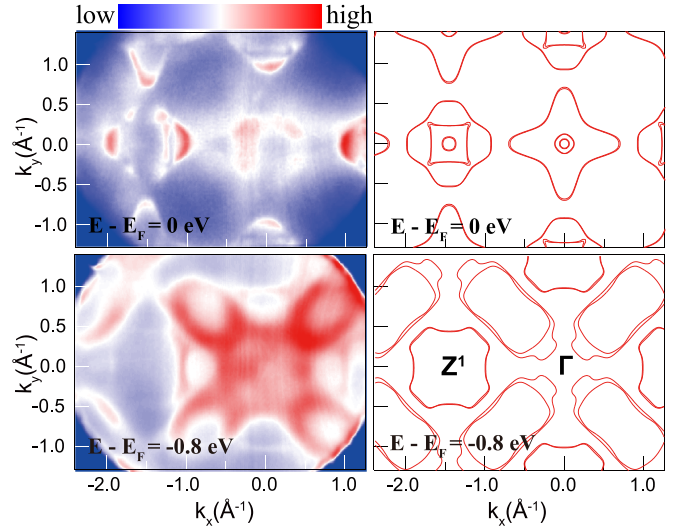


FIG. 2. Left: constant energy contours at  $E = 0$  and  $-0.8$  eV using 150 eV photons at 5.2 K. Right: the corresponding DFT calculations.

be found in Refs. [37–42]. Note that, for the ARPES spectra presented in this paper, core level scans reveal dominant peaks from Ge, implying that the surface might be Ge terminated (Fig. S1 in [37]).

The  $k_x - k_z$  and  $k_x - k_y$  FS maps from ARPES measurements are summarized in Figs. 1(d) and 1(e), which reveal diamond-shaped FS pockets centered at the bulk  $\Gamma$  and Z points [Fig. 1(e)], respectively, with a periodicity in good accordance with the bulk BZ. A detailed photon-energy dependent study also shows well-defined  $k_z$  periodicity of the observed bands [Fig. 1(d)], which allows us to obtain an estimated inner potential of  $\sim 15$  eV. Hence the 120 eV and 150 eV photon-energy scans correspond to  $k_z \sim \pi$  and 0 [red dashed curves in Fig. 1(d)], respectively. The energy-momentum dispersions are displayed in Fig. 1(f), where the non-4*f* conduction bands from density-functional theory (DFT) calculations in the paramagnetic state are overlaid on top. The DFT calculations treat 4*f* electrons as core electrons and can provide a reasonable description of the observed conduction bands away from the Fermi level ( $E_F$ ). However, the agreement near  $E_F$  is not satisfactory, due to correlation effects from Ce 4*f* electrons (see below). We note that theoretical calculations predict a very small band splitting and Weyl points in the band structure as a result of the noncentrosymmetric crystal structure [34], but such splitting is too small to be resolved in our data.

A detailed comparison between the ARPES constant-energy maps and DFT calculations is shown in Fig. 2 (see Fig. S2 in [37] for more details). DFT calculations predict two hole pockets and one tiny electron pocket at Z, as well as one large electron pocket and two small hole pockets at  $\Gamma$ , which partially agree with experiments, although some small pockets are absent experimentally [see also Fig. 1(f)]. In general, the constant energy maps away from  $E_F$  show better agreement with DFT calculations, compared to those close to  $E_F$ , reflecting the strong local correlations of the 4*f* electrons, which usually affect the quasiparticle dispersion only in the

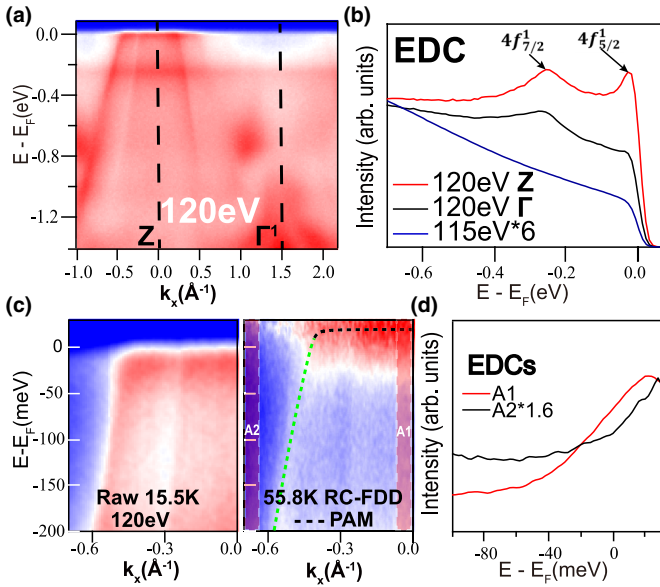


FIG. 3. (a) Band dispersion along  $\Gamma$ -Z from resonant ARPES. (b) Resonant EDCs from the black dashed cuts in (a), together with the off-resonant EDC at 115 eV. (c) Left: zoom-in view of the quasi-particle dispersion at 15.5 K near  $E_F$ . Right: the 56 K data divided by the RC-FDD. The dotted curve is the fitted band dispersion using Eq. (1). (d) Two integrated EDCs from the RC-FDD-divided 56 K data, for two momentum regions (A1 and A2) marked in (c).

vicinity of  $E_F$ . A previous de Haas–van Alphen (dHvA) effect study at very low temperatures indicates that the FS shape of CeCoGe<sub>3</sub> is overall similar to that of LaCoGe<sub>3</sub> with only small differences [43], while the cyclotron mass of the dominant dHvA branch is ten times higher for CeCoGe<sub>3</sub> ( $\sim 10m_e$  for CeCoGe<sub>3</sub> vs  $\sim 1m_e$  for LaCoGe<sub>3</sub>). This implies that although the overall FS shape of CeCoGe<sub>3</sub> is not significantly altered by the 4*f* electrons, appreciable contributions from 4*f* electrons are present in the FS due to the Kondo effect.

To probe the 4*f* states, we performed resonant ARPES measurements at the Ce *N* edge near 120 eV, which significantly enhances the 4*f* contribution to the measured spectra. The resonant ARPES spectrum [Fig. 3(a)] features a flat 4*f* band right at  $E_F$  near the Z point. This is better illustrated by the energy distribution curves (EDCs) shown in Fig. 3(b), where clear resonance enhancement of the peaks at  $E_F$  and  $-0.25$  eV can be observed, corresponding to the  $4f_{5/2}^1$  and  $4f_{7/2}^1$  peaks, respectively [44,45]. Although the  $4f_{7/2}^1$  peak can be clearly observed at all momentum points, the  $4f_{5/2}^1$  peak exhibits a large momentum dependence (see Fig. S3 in [37] for detailed FS maps). In particular, the absence of a  $4f_{5/2}^1$  peak around the  $\Gamma$  point may be attributed to a small indirect gap as a result of hybridization between conduction and 4*f* electrons (*c* – *f* hybridization). The *c* – *f* hybridization can also give rise to weak band bending near  $E_F$  [14,46–50], as shown in Fig. 3(c). To reveal the fine dispersion near  $E_F$ , we divide the ARPES spectra at 56 K by the resolution-convoluted Fermi-Dirac distribution (RC-FDD), obtained by fitting the reference spectrum. The result [right panel in Fig. 3(c)] reveals a weakly dispersive 4*f* band whose center lies slightly

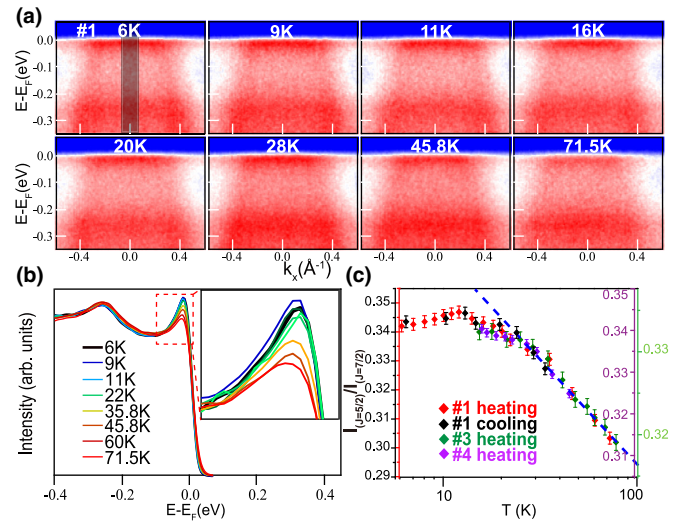


FIG. 4. (a) Resonant ARPES spectra near Z at various temperatures for a typical sample (no. 1). (b) The temperature-dependent EDCs obtained by integrating the shaded region in (a). Inset is an enlarged view of the  $4f_{5/2}^1$  peak. (c) The ratio between the integrated intensity of  $4f_{5/2}^1$  [ $-0.09$  eV,  $0$  eV] and that of  $4f_{7/2}^1$  [ $-0.38$  eV,  $-0.12$  eV], as a function of temperature. The blue dashed curve indicates the  $-\log(T)$  reference line. Note the slightly different vertical scales due to sample variation.

above  $E_F$ . For quantitative analysis, we adopted the hybridized band approach within the periodic Anderson model (PAM), where the band dispersion can be described by

$$E^\pm(k) = \frac{\bar{\epsilon}_f + \epsilon_k \pm \sqrt{(\bar{\epsilon}_f - \epsilon_k)^2 + 4V^2}}{2}. \quad (1)$$

Here,  $\bar{\epsilon}_f$  and  $\epsilon_k$  are the energies of the single-ion  $4f_{5/2}^1$  Kondo resonance and the conduction band in the absence of *c* – *f* hybridization, respectively, and *V* is the effective *c* – *f* hybridization strength. Our analysis is focused on the lower-energy branch in Eq. (1), which crosses  $E_F$ , and we assume that  $\epsilon_k$  is linear in *k* in the vicinity of  $E_F$ . The peak positions can be obtained by analyzing the momentum distribution curves (MDCs) and EDCs (Fig. S4 in [37]), which can then be fitted by Eq. (1) to obtain  $V \sim 10$  meV, indicating a moderate *c* – *f* hybridization. The RC-FDD divided EDCs in Fig. 3(d) further reveal clear momentum dependence of the positions of the 4*f* bands (hence an indirect gap caused by the *c* – *f* hybridization), which could explain the very weak  $4f_{5/2}^1$  peak far away from Z.

Temperature-dependent ARPES measurements near the Z point are summarized in Figs. 4(a) and 4(b). We first note that the  $4f_{5/2}^1$  peak can already be observed at  $\sim 80$  K (and above), similar to other HF systems [48,49,51], implying that Kondo screening takes place already at high temperatures, presumably involving excited crystal field states. Upon cooling, the  $4f_{5/2}^1$  peak becomes more prominent due to the gradual buildup of heavy quasiparticles from the Kondo effect, while the  $4f_{7/2}^1$  peak at  $-0.25$  eV remains largely unchanged, probably due to its much higher state degeneracy (hence higher  $T_K$ ) [52,53]. In Fig. 4(c), we plot the temperature

evolution of the relative intensity of the  $4f_{5/2}^1$  peak, i.e., the ratio between the integrated intensity of  $4f_{5/2}^1$  and that of  $4f_{7/2}^1$ , which reduces extrinsic effects that might affect the normalization of the temperature-dependent data (see Fig. S5 in [37] for details). The relative  $4f_{5/2}^1$  intensity roughly follows a  $-\log(T)$  behavior from  $\sim 25$  K and above, as expected for a Kondo peak in the paramagnetic state [48,49], but it increases more slowly upon cooling below  $T_1 \sim 25$  K and eventually ceases to grow below  $T_2 \sim 12$  K. We emphasize that such a temperature evolution has been confirmed by measurements from different samples (Fig. S6 in [37]), as well as in different cooling and warming cycles from the same sample. The results indicate that the heavy quasiparticle formation due to the Kondo effect begins to slow down below  $T_1$  and stops (or becomes slightly suppressed) below  $T_2$ . The fact that  $T_1$  is close to  $T_{N1} = 21$  K implies that the weakening of the Kondo processes is very likely caused by the development of long-range AFM order. Our results therefore show that the magnetic order and Kondo screening coexist and compete over a large temperature window, even deep inside the AFM phase.

Our observation is in stark contrast to those from previous ARPES measurements of the Ce-based AFM Kondo systems  $\text{CeRh}_2\text{Si}_2$  and  $\text{CePt}_2\text{In}_7$ . For the former with a very high  $T_N = 42$  K, the Kondo peak from ARPES measurements shows a monotonic increase with cooling, without any noticeable deviation even well below  $T_N$  [30]. For  $\text{CePt}_2\text{In}_7$ , the suppression of a weak Kondo peak occurs below  $\sim 60$  K [54], much higher than  $T_N = 5$  K, which, however, is different from the results inferred from Knight shift measurements which imply a relocation of the  $4f$  electrons only below  $\sim 12$  K [55]. We note that recent ARPES studies on the  $5f$ -electron compounds  $\text{USb}_2$  and  $\text{UAs}_2$  show that the magnetic order and Kondo effect could coexist without interfering with each other [56,57]. Specifically, ARPES measurements revealed two sets of  $5f$ -derived quasiparticle bands that are well separated in momentum space [56,57]: in one band, the itinerant SDW order opens up a gap (hence accounting for the magnetism), while the other band corresponds to the typical heavy quasiparticles found in HF systems where the peak intensity remains unaffected by the development of AFM order. The differences between the U-based and Ce-based compounds could be attributed to the different number of  $f$  electrons: in U-based compounds, U normally has three electrons in the  $5f$  orbitals which may selectively participate in the Kondo screening or AFM order; by contrast, in Ce there is only one electron in the  $4f$  shell, so that such orbital selectivity is not possible. Therefore, in Ce-based HF materials, the competition and coexistence of Kondo effect and AFM order must be of a fundamentally different nature.

The origin of this competing behavior in  $\text{CeCoGe}_3$  may lie in the localized nature of the  $4f$ -electron magnetism, namely, the AFM order consists of Ising-like moments pointing along  $z$  that are coupled ferromagnetically in the  $x-y$  plane and antiferromagnetically along the  $z$  direction with different ordering vectors  $\mathbf{k} = (0, 0, q_z)$  in the three magnetic phases [33]. The commensurate AFM orderings in  $\text{CeCoGe}_3$  are unlikely to correspond to the itinerant SDW type and the observed FS does not show obvious sign of nesting. In

addition, temperature-dependent FS mappings do not reveal any significant change in the FS shape across the AFM transitions (Fig. S7 in [37]), supporting the local-moment nature of the AFM order. Note that the cleaved surface is most likely to be Ge-terminated based on core level analysis, which implies that the observed  $4f$  states should be close to the bulk. On the other hand, since no clear reconstruction of the electronic structure is observed across the AFM transitions, how surface effects could affect the spectral changes remains an open question.

The observation of coexistence and competition between the magnetic order and the Kondo effect in Fig. 4(c) poses the question as to the nature of the microscopic interplay between these phenomena. One possible scenario is that both the ordered magnetic moments and Kondo screening are modulated in real space, such that there is a periodic arrangement of sizable ordered moments and Kondo-screened moments. Such a picture was also proposed based on a previous neutron scattering study [58], while an analogous proposal was put forward for  $\text{UAs}_2$  based on a two-channel Kondo model for multiple  $5f$  electrons [59]. Such a scenario could account for the significant Kondo weight persisting well below  $T_N$ , while the close interplay between the magnetic structure and Kondo screening may also explain why the turning point  $T_2$  is close to  $T_{N2}$  (and  $T_{N3}$ ), where there is a change of magnetic structure [33].

Interestingly, for the experimental  $k_x - k_z$  map in Fig. 1(d), the dominant pocket observed near  $Z$  has a Fermi vector  $k_F$  [marked by a green arrow in Fig. 1(d)] that is approximately  $1/2$  of  $\Gamma$ - $Z$ . Therefore, the oscillatory RKKY interaction along  $z$  could have a node for interactions between nearest-neighbor Ce planes (note that for the body-centered structure there are two Ce atoms per conventional unit cell separated by  $c/2$  along  $z$  [Fig. 1(a)]). Below  $T_{N3}$ , where  $q_z = 1/2$ , the AFM order could lead to adjacent Ce layers alternating between large ordered moments (antiparallel between next-nearest layers) and nearly zero moments (Kondo screened) (Fig. S8 in [37]). Note that, although a “two-up two-down” magnetic structure was previously proposed based on the assumption of equal moments [33], the neutron diffraction results are equally compatible with the modulated structure described here, after a shift of the global phase by  $\pi/4$ .

An alternative scenario would be that there is an inherent on-site competition and coexistence of magnetic order and Kondo screening, if the real-space modulation is absent. In this case, the Kondo weight is expected to decrease inside the AFM phase or even reach zero in the zero-temperature limit if the AFM QCP is of the local type [1,2,14,15,60]. Although the current results suggest a very small decrease of Kondo weight below  $T_2$  [Fig. 4(c)], the weight appears to remain finite based upon a simple extrapolation to lower temperatures. On the other hand, since the current measurements are performed only down to 6 K, determining the fate of the Kondo peak in the zero-temperature limit requires future measurements to significantly lower temperatures.

To conclude, using high-resolution ARPES, we probed the quasiparticle bands near  $E_F$  in  $\text{CeCoGe}_3$  with a high  $T_{N1} = 21$  K. The presence of a well-resolved heavy  $4f$  band with a relatively simple momentum distribution allows us to clearly track the temperature evolution of the  $4f$  band across

the AFM transitions and we find that its intensity starts to deviate from the typical  $-\log(T)$  behavior just above  $T_{N1}$  and eventually ceases to grow at lower temperatures. Our results provide direct spectroscopic evidence for the competition between the well-localized magnetic order and Kondo effect in a HF system, which might be related to a real-space modulation of magnetic moments and Kondo screening. These findings may be useful for understanding other HF systems with local-moment antiferromagnetism, e.g., CeRhIn<sub>5</sub>, where a “small FS” with enhanced cyclotron masses is observed below  $T_N$  from dHvA measurements [61,62], while ARPES reveals weakly dispersive  $4f$  bands well above  $T_N$  from moderate  $c-f$  hybridization [63], similar to CeCoGe<sub>3</sub>. Nevertheless, the low ordering temperature of  $T_N = 3.8$  K in CeRhIn<sub>5</sub> has precluded direct observation of such competition. Finally, since the degree of  $f$ -electron itinerancy and the nature of the magnetic ground state can be readily tuned by elemental substitution in the CeTX<sub>3</sub> series [43,64–68], these systems could be ideal candidates for systematically studying the electronic manifestation of the competition between the RKKY and Kondo interactions.

This work is supported by the State Key project of Zhejiang Province (Grant No. LZ22A040007), the Key R&D Program of Zhejiang Province, China (Grant No. 2021C01002), NSF of China (Grants No. 12174331, No. 12034017, No. U2032208, No. 12174332, No. 11974397, and No. 12222410), National Key R&D Program of the MOST of China (Grants No. 2022YFA1402200 and No. 2017YFA0303100), Zhejiang Provincial Natural Science Foundation of China (Grant No. LR22A040002), the Fundamental Research Funds for the Central Universities (Grant No. 2021FZZX001-03), and Bridging Grants with China, Japan, South Korea, and ASEAN region (No. BG11-072020) funded by the Swiss State Secretariat. Part of this research used Beamline 03U at SSRF, supported by ME2 project under Contract No. 11227902 from NSF of China. The work at the University of Warwick was supported by EPSRC, UK, through Grants No. EP/M028771/1 and No. EP/T005963/1. J.K. was supported in part by the Deutsche Forschungsgemeinschaft through the Cluster of Excellence ML4Q (Grant No. 90534769). We thank Dr. S. Wu for helpful discussions on the previous neutron results.

- 
- [1] P. Coleman, *Heavy Fermions: Electrons at the Edge of Magnetism. Handbook of Magnetism and Advanced Magnetic Materials*, Vol. 1 (Wiley, New York, 2007).
- [2] P. Gegenwart, Q. Si, and F. Steglich, *Nat. Phys.* **4**, 186 (2008).
- [3] H. v. Löhneysen, A. Rosch, M. Vojta, and P. Wölfle, *Rev. Mod. Phys.* **79**, 1015 (2007).
- [4] S. Sachdev, *Quantum Phase Transitions* (Cambridge University Press, Cambridge, UK, 2011).
- [5] F. Steglich, J. Aarts, C. D. Bredl, W. Lieke, D. Meschede, W. Franz, and H. Schäfer, *Phys. Rev. Lett.* **43**, 1892 (1979).
- [6] N. D. Mathur, F. M. Grosche, S. R. Julian, I. R. Walker, D. M. Freye, R. K. W. Haselwimmer, and G. G. Lonzarich, *Nature (London)* **394**, 39 (1998).
- [7] G. R. Stewart, *Rev. Mod. Phys.* **73**, 797 (2001).
- [8] M. A. Ruderman and C. Kittel, *Phys. Rev.* **96**, 99 (1954).
- [9] T. Kasuya, *Prog. Theor. Phys.* **16**, 45 (1956).
- [10] K. Yosida, *Phys. Rev.* **106**, 893 (1957).
- [11] J. Kondo, *Prog. Theor. Phys.* **32**, 37 (1964).
- [12] A. C. Hewson, *The Kondo Problem to Heavy Fermions* (Cambridge University Press, Cambridge, UK, 1993).
- [13] A. Nejtati, K. Ballmann, and J. Kroha, *Phys. Rev. Lett.* **118**, 117204 (2017).
- [14] S. Kirchner, S. Paschen, Q. Chen, S. Wirth, D. Feng, J. D. Thompson, and Q. Si, *Rev. Mod. Phys.* **92**, 011002 (2020).
- [15] Y.-f. Yang and D. Pines, *Proc. Natl. Acad. Sci. USA* **109**, E3060 (2012).
- [16] S. Doniach, *Physica B+C* **91**, 231 (1977).
- [17] G. Zwirnagl and U. Pulst, *Phys. B: Condens. Matter* **186-188**, 895 (1993).
- [18] P. Gegenwart, C. Langhammer, C. Geibel, R. Helfrich, M. Lang, G. Sparn, F. Steglich, R. Horn, L. Donnevert, A. Link, and W. Assmus, *Phys. Rev. Lett.* **81**, 1501 (1998).
- [19] O. Stockert, E. Faulhaber, G. Zwirnagl, N. Stüßer, H. S. Jeevan, M. Deppe, R. Borth, R. Küchler, M. Loewenhaupt, C. Geibel, and F. Steglich, *Phys. Rev. Lett.* **92**, 136401 (2004).
- [20] J. Arndt, O. Stockert, K. Schmalzl, E. Faulhaber, H. S. Jeevan, C. Geibel, W. Schmidt, M. Loewenhaupt, and F. Steglich, *Phys. Rev. Lett.* **106**, 246401 (2011).
- [21] Z. Wu, Y. Fang, H. Su, W. Xie, P. Li, Y. Wu, Y. Huang, D. Shen, B. Thiagarajan, J. Adell, C. Cao, H.-Q. Yuan, F. Steglich, and Y. Liu, *Phys. Rev. Lett.* **127**, 067002 (2021).
- [22] Q. Si, S. Rabello, K. Ingersent, and J. L. Smith, *Nature (London)* **413**, 804 (2001).
- [23] P. Coleman, C. Pépin, Q. Si, and R. Ramazashvili, *J. Phys.: Condens. Matter* **13**, R723 (2001).
- [24] J. Custers, P. Gegenwart, H. Wilhelm, K. Neumaier, Y. Tokiwa, O. Trovarelli, C. Geibel, F. Steglich, C. Pépin, and P. Coleman, *Nature (London)* **424**, 524 (2003).
- [25] H. Shishido, R. Settai, H. Harima, and Y. Ōnuki, *J. Phys. Soc. Jpn.* **74**, 1103 (2005).
- [26] T. Park, F. Ronning, H.-Q. Yuan, M. B. Salamon, R. Movshovich, J. L. Sarrao, and J. D. Thompson, *Nature (London)* **440**, 65 (2006).
- [27] S. Friedemann, N. Oeschler, S. Wirth, C. Krellner, C. Geibel, F. Steglich, S. Paschen, S. Kirschner, and Q. Si, *Proc. Natl. Acad. Sci. USA* **107**, 14547 (2010).
- [28] J. Bork, Y.-h. Zhang, L. Diekhöner, L. Borda, P. Simon, J. Kroha, P. Wahl, and K. Kern, *Nat. Phys.* **7**, 901 (2011).
- [29] H. Prüser, P. E. Dargel, M. Bouhassoune, R. G. Ulbrich, T. Pruschke, S. Lounis, and M. Wenderoth, *Nat. Commun.* **5**, 5417 (2014).
- [30] G. Poelchen, S. Schulz, M. Mende, M. Güttler, A. Generalov, A. V. Fedorov, N. Caroca-Canales, C. Geibel, K. Kliemt, C. Krellner, S. Danzenbächer, D. Yu. Usachov, P. Dudin, V. N. Antonov, J. W. Allen, C. Laubschat, K. Kummer, Y. Kucherenko, and D. V. Vyalikh, *npj Quantum Mater.* **5**, 70 (2020).

- [31] V. K. Pecharsky, O.-B. Hyun, and K. A. Gschneidner, *Phys. Rev. B* **47**, 11839 (1993).
- [32] A. Thamizhavel, T. Takeuchi, T. D. Matsuda, Y. Haga, K. Sugiyama, R. Settai, and Y. Ōnuki, *J. Phys. Soc. Jpn.* **74**, 1858 (2005).
- [33] M. Smidman, D. T. Adroja, A. D. Hillier, L. C. Chapon, J. W. Taylor, V. K. Anand, R. P. Singh, M. R. Lees, E. A. Goremychkin, M. M. Koza, V. V. Krishnamurthy, D. M. Paul, and G. Balakrishnan, *Phys. Rev. B* **88**, 134416 (2013).
- [34] V. Ivanov, X. Wan, and S. Y. Savrasov, *Phys. Rev. B* **103**, L041112 (2021).
- [35] R. Settai, I. Sugitani, Y. Okuda, A. Thamizhavel, M. Nakashima, Y. Ōnuki, and H. Harima, *J. Magn. Magn. Mater.* **310**, 844 (2007).
- [36] P. A. Frigeri, D. F. Agterberg, A. Koga, and M. Sigrist, *Phys. Rev. Lett.* **92**, 097001 (2004).
- [37] See Supplemental Material at <http://link.aps.org/supplemental/10.1103/PhysRevB.107.L201104> for as well as ARPES measurement details and additional experimental data and analysis, which includes Refs. [38–42].
- [38] Y.-C. Yang, Z.-T. Liu, J.-S. Liu, Z.-H. Liu, W.-L. Liu, X.-L. Lu, H.-P. Mei, A. Li, M. Ye, S. Qiao, and D.-W. Shen, *Nuc. Sci. Tech.* **32**, 31 (2021).
- [39] G. Kresse and J. Hafner, *Phys. Rev. B* **47**, 558 (1993).
- [40] G. Kresse and D. Joubert, *Phys. Rev. B* **59**, 1758 (1999).
- [41] J. P. Perdew, K. Burke, and M. Ernzerhof, *Phys. Rev. Lett.* **77**, 3865 (1996).
- [42] A. A. Mostofi, J. R. Yates, Y.-S. Lee, I. Souza, D. Vanderbilt, and N. Marzari, *Comput. Phys. Commun.* **178**, 685 (2008).
- [43] A. Thamizhavel, H. Shishido, Y. Okuda, H. Harima, T. D. Matsuda, Y. Haga, R. Settai, and Y. Ōnuki, *J. Phys. Soc. Jpn.* **75**, 044711 (2006).
- [44] J. W. Allen, *J. Phys. Soc. Jpn.* **74**, 34 (2005).
- [45] A. Sekiyama, T. Iwasaki, K. Matsuda, Y. Saitoh, Y. Ōnuki, and S. Suga, *Nature (London)* **403**, 396 (2000).
- [46] H. J. Im, T. Ito, H.-D. Kim, S. Kimura, K. E. Lee, J. B. Hong, Y. S. Kwon, A. Yasui, and H. Yamagami, *Phys. Rev. Lett.* **100**, 176402 (2008).
- [47] S. Patil, A. Generalov, M. Güttler, P. Kushwaha, A. Chikina, K. Kummer, T. C. Rödel, A. F. Santander-Syro, N. Caroca-Canales, C. Geibel, S. Danzenbächer, Y. Kucherenko, C. Laubschat, J. W. Allen, and D. V. Vyalikh, *Nat. Commun.* **7**, 11029 (2016).
- [48] Q. Y. Chen, D. F. Xu, X. H. Niu, J. Jiang, R. Peng, H. C. Xu, C. H. P. Wen, Z. F. Ding, K. Huang, L. Shu, Y. J. Zhang, H. Lee, V. N. Strocov, M. Shi, F. Bisti, T. Schmitt, Y. B. Huang, P. Dudin, X. C. Lai, S. Kirchner *et al.*, *Phys. Rev. B* **96**, 045107 (2017).
- [49] S. Y. Jang, J. D. Denlinger, J. W. Allen, V. S. Zapf, M. B. Maple, J. N. Kim, B. G. Jang, and J. H. Shim, *Proc. Natl. Acad. Sci. USA* **117**, 23467 (2020).
- [50] Y. Wu, Y. Zhang, F. Du, B. Shen, H. Zheng, Y. Fang, M. Smidman, C. Cao, F. Steglich, H. Yuan, J. D. Denlinger, and Y. Liu, *Phys. Rev. Lett.* **126**, 216406 (2021).
- [51] D. Ehm, S. Hübner, F. Reinert, J. Kroha, P. Wölfle, O. Stockert, C. Geibel, and H. v. Löhneysen, *Phys. Rev. B* **76**, 045117 (2007).
- [52] F. Reinert, D. Ehm, S. Schmidt, G. Nicolay, S. Hübner, J. Kroha, O. Trovarelli, and C. Geibel, *Phys. Rev. Lett.* **87**, 106401 (2001).
- [53] J. Kroha, S. Kirchner, G. Sellier, P. Wölfle, D. Ehm, F. Reinert, S. Hübner, and C. Geibel, *Phys. E* **18**, 69 (2003).
- [54] Y. Luo, C. Zhang, Q.-Y. Wu, F.-Y. Wu, J.-J. Song, W. Xia, Y. Guo, J. Rusz, P. M. Oppeneer, T. Durakiewicz, Y.-Z. Zhao, H. Liu, S.-X. Zhu, Y.-H. Yuan, X.-F. Tang, J. He, S.-Y. Tan, Y.-B. Huang, Z. Sun, Y. Liu *et al.*, *Phys. Rev. B* **101**, 115129 (2020).
- [55] N. apRoberts-Warren, A. P. Dioguardi, A. C. Shockley, C. H. Lin, J. Crocker, P. Klavins, D. Pines, Y.-F. Yang, and N. J. Curro, *Phys. Rev. B* **83**, 060408(R) (2011).
- [56] Q. Y. Chen, X. B. Luo, D. H. Xie, M. L. Li, X. Y. Ji, R. Zhou, Y. B. Huang, W. Zhang, W. Feng, Y. Zhang, L. Huang, Q. Q. Hao, Q. Liu, X. G. Zhu, Y. Liu, P. Zhang, X. C. Lai, Q. Si, and S. Y. Tan, *Phys. Rev. Lett.* **123**, 106402 (2019).
- [57] X. Ji, X. Luo, Q. Chen, W. Feng, Q. Hao, Q. Liu, Y. Zhang, Y. Liu, X. Wang, S. Tan, and X. Lai, *Phys. Rev. B* **106**, 125120 (2022).
- [58] S. Wu, Ph.D. thesis, Johns Hopkins University, 2017.
- [59] C. D. O. Neill, J. L. Schmeh, H. D. J. Keen, L. P. Cairns, D. A. Sokolov, A. Hermann, D. Wermeille, P. Manuel, F. Krüger, and A. D. Huxley, *Proc. Natl. Acad. Sci. USA* **118**, e2101148118 (2021).
- [60] J. Kroha, [arXiv:1710.00192](https://arxiv.org/abs/1710.00192).
- [61] H. Shishido, R. Settai, D. Aoki, S. Ikeda, H. Nakawaki, N. Nakamura, T. Iizuka, Y. Inada, K. Sugiyama, T. Takeuchi, K. Kindo, T. C. Kobayashi, Y. Haga, H. Harima, Y. Aoki, T. Namiki, H. Sato, and Y. Ōnuki, *J. Phys. Soc. Jpn.* **71**, 162 (2002).
- [62] N. Harrison, U. Alver, R. G. Goodrich, I. Vekhter, J. L. Sarrao, P. G. Pagliuso, N. O. Moreno, L. Balicas, Z. Fisk, D. Hall, R. T. Macaluso, and J. Y. Chan, *Phys. Rev. Lett.* **93**, 186405 (2004).
- [63] Q. Y. Chen, D. F. Xu, X. H. Niu, R. Peng, H. C. Xu, C. H. P. Wen, X. Liu, L. Shu, S. Y. Tan, X. C. Lai, Y. J. Zhang, H. Lee, V. N. Strocov, F. Bisti, P. Dudin, J.-X. Zhu, H. Q. Yuan, S. Kirchner, and D. L. Feng, *Phys. Rev. Lett.* **120**, 066403 (2018).
- [64] Y. Okuda, Y. Miyauchi, Y. Ida, Y. Takeda, C. Tonohiro, Y. Oduchi, T. Yamada, N. Duc Dung, T. D. Matsuda, Y. Haga, T. Takeuchi, M. Hagiwara, K. Kindo, H. Harima, K. Sugiyama, R. Settai, and Y. Ōnuki, *J. Phys. Soc. Jpn.* **76**, 044708 (2007).
- [65] T. Terashima, M. Kimata, S. Uji, T. Sugawara, N. Kimura, H. Aoki, and H. Harima, *Phys. Rev. B* **78**, 205107 (2008).
- [66] T. Ohkochi, T. Toshimitsu, H. Yamagami, S. Fujimori, A. Yasui, Y. Takeda, T. Okane, Y. Saitoh, A. Fujimori, Y. Miyauchi, Y. Okuda, R. Settai, and Y. Ōnuki, *J. Phys. Soc. Jpn.* **78**, 084802 (2009).
- [67] M. Smidman, D. T. Adroja, E. A. Goremychkin, M. R. Lees, D. M. Paul, and G. Balakrishnan, *Phys. Rev. B* **91**, 064419 (2015).
- [68] J. Pásztorová, A. Howell, M. Songvilay, P. M. Sarte, J. A. Rodriguez-Rivera, A. M. Arévalo-López, K. Schmalzl, A. Schneidewind, S. R. Dunsiger, D. K. Singh, C. Petrovic, R. Hu, and C. Stock, *Phys. Rev. B* **99**, 125144 (2019).